Scilight

Photochemistry and Spectroscopy
https://www.sciltp.com/journals/ps

Article

Check for updates

Assessment of Structural Changes in Burned Bones Remains: The Role of Raman Spectroscopy †

Alberto Milani [1], Luigi Brambilla [1], Victor Hernandez Jolin [2], Cecilio Barroso [2], Cristina Capel Ferrón [2], José L. Zafra [2] and Mirella Del Zoppo [1,*]

[1] Department of Chemistry, Materials and Chemical Engineering, Polytechnic Milan, 20133 Milano, Italy
[2] Department of Physical Chemistry, University of Malaga, Avda. Cervantes, 2, 29071 Malaga, Spain
* Correspondence: mirella.delzoppo@polimi.it
† This article is dedicated to Prof. Giuseppe Zerbi in recognition of his outstanding scientific contributions to Spectroscopy.

How To Cite: Milani, A.; Brambilla, L.; Jolin, V.H.; et al. Assessment of Structural Changes in Burned Bones Remains: The Role of Raman Spectroscopy. *Photochemistry and Spectroscopy* **2026**, *2*(2), 8. https://doi.org/10.53941/ps.2026.100019

Received: 15 December 2025
Revised: 1 April 2026
Accepted: 3 April 2026
Published: 1 June 2026

Abstract: The analysis of burned bones, both for archaeological or forensic purposes, can be highly informative of the history of these remains. For this reason, analytical tools are highly desirable. Among the most widely used techniques, vibrational spectroscopy plays an important role for the ease of application and the wealth of information it can provide. Both FTIR absorption and Raman scattering techniques can be used and several crystallinity-index-calculating methods have been proposed. In this work we show that Raman spectroscopy offers reliable crystallinity markers which yield results consistent with those obtained with IR. Moreover, Raman spectroscopy does not require complex or invasive sampling procedures and possibly enables "*in situ*" measurements thanks to the use of portable instruments.

Keywords: Raman spectroscopy; FTIR (Fourier-Transform InfraRed); Burned bones; crystallinity index

1. Introduction

The mineral phase of bones, which accounts for 60–70 weight% [1], can be referred to as a carbonate substituted hydroxyapatite named bioapatite. Many possibilities of substitution can occur in this phase leading to a poorly crystalline form of hydroxyapatite, with small sized crystals and a high structural strain. A number of genetic and nongenetic factors can alter the mineral composition. One of the most significant changes to the structure and composition of bone occurs when this material is heated. Heated bone is one of the most challenging osteological materials to study, since the process of heating produces complicated changes within the material such as dehydration, loss of the organic component, coalescence of crystal structure, etc. [2–4].

Analysis of skeletal remains burned under controlled laboratory conditions at different temperatures has enabled the development of different methods to estimate the thermal history of the bones. This is of particular relevance in the case of archaeology even if fossil bones present important modifications with respect to fresh, unaltered bones. These changes can produce modifications of color, appearance of new constituent minerals (recrystallized hydroxyapatite, whitlockite) and changes in the crystallinity of phosphatic phases [5,6]

In particular, heating is known to lead to an increased crystallite size and a decreased lattice strain [7] which need to be monitored in order to derive useful information on the history of the remains. Different spectroscopic techniques can be used to this purpose and several markers such as the crystallinity index and other spectroscopic markers (see e.g., [8,9]) have been discussed in the literature and widely used.

The crystalline index is a measure of the crystal order, strain and organization in bone. When bone is fresh, the bulk structure is poorly crystalline [8], partly as a result of carbonate substitution causing crystal disorder [1].

Crystallinity throughout the skeleton of the human body is not uniform, and it varies among the different mineralized tissues [10]. Age has been shown to have an influence on crystallinity, with younger bones being less crystalline than more mature bones [11]. There are also species differences in bone mineral crystallinity, although some of these relate more to differences in the proportion of organic material within rather than species difference per se [12].

As a result of heating and burning, the crystal structure of bone becomes better ordered and characterized by larger crystals and less strain, and as such the CI value increases [4].

According to Etok et al. [4] there are three key stages:

(i) 25–250 °C: loss of loosely bound water up to 100 °C, with little change in organic and mineral matrices, followed by loss of structural water within protein and mineral-surface bound water up to 250 °C;
(ii) 300–500 °C: combustion of organic component (50–55% mass loss), associated with increase in mean crystallite size from 10 nm to 30 nm, and an increase in crystallite thickness from 2 nm to 8–9 nm, together with formation of new mineral phases (buchwaldite, halite, sylvite);
(iii) above 500 °C: any residual organic matter, is burnt off, and mean crystallite size progressively increases as well as crystallite thickness. A further phase, β-tricalcium phosphate, appears at 900 °C.

Given this brief and necessarily incomplete description of the extremely complex nature of the problem it is evident that it is mandatory to have reliable characterization tools. Several techniques have been used to this aim. In this work we focus on the use of vibrational spectroscopy and in particular on Raman scattering.

The key point in the characterization of burned bones is the determination of the crystallinity index.

The CI can be calculated, e.g., using X-ray Diffraction (XRD), Fourier Transform InfraRed spectroscopy (FTIR) and Raman spectroscopy, although the specific calculations and values will differ between the different techniques. As a result, CI values from the various methods are not directly comparable, although the general trends are similar. Each one of these techniques has its own advantages. CI value as determined from X ray-analysis (X-ray CI), rises in the early stages of diagenesis and is due to thermal events. Values reported in the scientific literature range between 0.00 and 0.57 [13].

In order to calculate CI using infrared spectroscopy the approach traditionally used is to measure the splitting factor (SF) of the two $(PO_4)^{3-}$ asymmetric bending vibrations bands peaked at ~605 cm^{-1} and ~565 cm^{-1} defined as the sum of the heights above baseline of the two bands divided by the height of the valley between the two bands at 595 cm^{-1}.

$$SF = I\ (565\ cm^{-1}) + I\ (605\ cm^{-1})/I\ (595\ cm^{-1})$$

It has been demonstrated that SF increases with the degree of crystallinity [14,15].

Great relevance has been given to the use of IR spectroscopy both in absorption (hereafter referred to as IR) and attenuated total reflection (ATR). For solid samples, as bone materials, IR spectroscopic analysis is commonly performed in KBr pellets. With this method, to obtain good and reliable spectra, a small amount of powdered sample mixed with KBr powders is subjected to mechanical grinding and sintering at 10 tons/cm^2. In principle, these operations might alter, to some extent, the crystal structure of the material. On the contrary, ATR is a spectroscopic straightforward method with remarkable potential for quick and easy sampling often requiring no demanding preparation of the samples. However, it is well known that an ATR spectrum differs from its transmission counterpart in band position, band shape and relative intensities all over the spectral range. These differences are related to the inherent way in which ATR works. It is worth remembering that ATR is based on the interaction between the electromagnetic evanescent wave at the surface of a high refractive index crystal and the sample which must be in conformal contact with it. In this experimental set-up the penetration depth of the IR light into the samples is small (1 to 3 μm) and depends on wavelength, incident angle, and refractive indices of the ATR crystal and sample. To compare ATR and transmission spectra appropriate correction algorithms are needed, but often they are not foolproof. For this reason, it is crucial to validate which approach can be used to confidently evaluate bone mineral crystallinity using vibrational spectroscopy. Many studies have tried to correlate different spectral IR features to the standard XRD measurement of crystallinity (see for example, [16]).

An alternative spectroscopic approach relies on the use of Raman spectroscopy which has, in principle, the advantage of not requiring any sample preparation and is not affected by the problems inherent with the IR techniques. Moreover, with portable Raman instrumentation, which to date has achieved notable performances, the analyses can be performed directly on site. One of the most widely used methods to estimate CI from Raman spectra is the reciprocal of the FWHM (Full Width at Half Maximum) of the 960 cm^{-1} Raman line ($\nu_1(PO_4)^{3-}$ symmetric stretching vibration).

To assess the reliability of the different markers which can be obtained using both IR and Raman spectroscopies, in this work, FT-Raman data recorded on samples of burned bones from an archaeologic excavation site, have been compared to results obtained with IR measurements.

2. Material and Methods

53 fragments of burned bones found in The Cueva del Angel (Lucena, Spain), an Acheulean hunter habitat in the South of the Iberian Peninsula have been studied by means of vibrational spectroscopy (both IR and Raman).

FT-Raman spectra of burned bones were recorded with a Nicolet NXR 9650 FT-Raman spectrometer coupled to a Thermo Microstage FT-Raman Microscope (both from Thermo Fischer Scientific, Waltham, MA, USA) (excitation laser wavelength 1064 nm, power on the sample 300 mW, and 512 scan). With the purpose of minimizing the possible inhomogeneity of the samples, bones were prepared in powder form, placed in a metallic cup and analyzed under the focusing mirror of the microstage with a 1 mm laser spot.

IR absorption spectra (in the following referred to as IR) of bones were recorded with a Nicolet Nexus FT-IR spectrometer on samples prepared in KBr pellets (128 scan, 4 cm^{-1}). These pellets have been obtained by mixing and finely grinding a few mg of powdered bone with 100–200 mg of spectroscopic grade potassium bromide (KBr) in an agate mortar. The fine powder obtained is then sintered at 10 ton/cm^2 into a transparent disk-shaped pellet.

Spectral data were obtained and processed with Thermo Fisher Scientific Inc. *OMNIC* 8.2.0.387 software.

The values of the full width at half maximum (FWHM) of Raman bands have been obtained by a curve fitting analysis of the spectra with *Fityk-1.3.1* program adopting Pseudovoigt functions [17].

3. Results and Discussion

The most widely used Raman spectroscopic marker used to characterize bones tissues is the so called Raman Crystallinity Index (Raman CI) obtained (i) as the reciprocal of the FWHM of the 960 cm^{-1} Raman line ($\nu_1(PO_4)^{3-}$ band symmetric stretching vibration) or (ii) as the carbonate to phosphate band intensities ratio. The rationale behind the former is the variation of the bandwidth with the degree of crystallinity which is believed to increase on exposure to higher temperatures [5]. A larger degree of crystallinity corresponds to a narrower Raman line. In the second case CI is calculated as the ratio of the integrated areas of the $\nu_1(CO_3)^{2-}$ band at 1085 cm^{-1}, to the $\nu_1(PO_4)^{3-}$ band at 960 cm^{-1}. An increase in temperature is expected to lead to a decrease of the carbonate/phosphate ratio due to carbonate loss [9]. In our case we prefer to focus on the former marker since due to strong fluorescence in some samples, the determination of the intensity of the phosphate band is often not straightforward.

Fluorescence is a well-known problem when considering Raman spectra. There are many different reasons for this to occur and it is one of the main limits of the technique. However, there are ways to, at least partially and in some circumstances, reduce the problem, e.g., change the exciting line, apply photobleaching, use UV resonance, etc.

In order to measure the Raman CI of our samples, we used an exciting laser line at 1064 nm because of the strong fluorescence emission, which almost completely obscures the Raman signal in some of the samples, when using visible 514 nm or near IR 785 nm laser lines. This in spite of several studies on fresh and burned bones, which in the literature use the 514 nm excitation (see for example [7]). The reason for the large fluorescence signal in our case is probably due to the nature of archaeological samples buried for thousands of centuries in a collapsed open air cave site [18] which could have been contaminated (e.g., ions uptake) or as a consequence of the burning process itself since during burning, the complex organic matrix of bone—primarily type I collagen—undergoes drastic chemical transformation. Under limited oxygen or controlled heating, it forms amorphous carbon, polycyclic aromatic hydrocarbons, and other graphite-like microcrystalline structures. Most of these carbonaceous products are highly fluorescent if excited by visible radiation.

A first very rough classification of the bone samples can be made by considering their color. Different coloration of fossil bones usually indicates that they have been subjected to some thermal events. Thus, the color of bones is the most commonly used characteristic to identify past occurrences of heating. The change in color depends on the temperature to which they were subjected [5]. In fact, several experimental studies are based on identifying the heating temperature from the color of the bones [19–21]. Dark colors indicate rather low temperatures [22], while white coloration indicates calcinations at relatively high temperatures [19]. Other studies show that color can vary enormously depending on certain intrinsic characteristics of fossil bones (e.g., thickness, presence or absence of organic matter), the color of sediments, the presence of organic acids or iron and manganese oxides [20,21,23]. However, the color of burned bones is still used as a general criterion for determining the combustion temperature to which bones have been subjected.

In this work we labeled the samples according to the color of the bone fragments, determined by eye, as W (white), B (black), YB (yellow/brown), BR (brown), R (red), LB (light brown), and G (gray).

The arbitrariness of the rough classification of the bone fragments considering by eye the color, is made evident when we examine the color of the powders obtained by soft mechanical grinding of the bones. The color of the powders is often different from that of the bone fragments and a classification of the color of the powders becomes even more erratic. This inconsistency might be due to contaminants mostly present on the surface of the bone (see for example Figure 1).

Figure 1. Change of color of a bone fragment (top) after mechanical grinding (bottom).

For the determination of the Raman CI, the FWHM of the 960 cm^{-1} line (see Figure 2a) has been measured. Given the intrinsically inhomogeneous nature of the samples examined, the reproducibility of the measurements is an issue. For this reason, two sets of measurements for each sample have been done (both spectra recording and band deconvolution). Indeed, in Figure 2b and in Table 1, we see that the correlation between the two sets of measurements is fair. In what follows the average value of the two measurements has been considered as FWHM.

Table 1. Values of the FWHM of the 960 cm^{-1} Raman line from set A, set B, and their average for 53 samples labelled as Wn = white, Bn = black, YBn = yellow-brown, BRn = brown, Rn = red, LBn = light brown and, Gn = grey where n is the progressive numbering in each group.

	W			B			YB			BR			R			LB			G		
n	**A**	**B**	**Average**	**A**	**B**	**Average**	**A**	**B**	**Average**	**A**	**B**	**Average**	**A**	**B**	**Average**	**A**	**B**	**Average**	**A**	**B**	**Average**
1	9.7	9.0	9.4	11.7	14.6	13.2	14.0	13.3	13.6	10.2	10.5	10.4	11.8	11.5	11.7	13.3	11.1	12.2	12.7	11.8	12.3
2	9.4	9.4	9.4	14.6	15.2	14.9	10.2	10.1	10.1	13.9	13.2	13.6	11.0	10.5	10.7	9.4	9.4	9.4	13.9	11.8	12.8
3	9.8	9.4	9.6	13.8	12.4	13.1	16.3	16.3	16.3	13.3	12.9	13.1	14.2	13.0	13.6	10.7	9.7	10.2	12.7	12.1	12.4
4	12.8	11.3	12.0	13.3	10.9	12.1	12.8	12.5	12.7	10.8	11.0	10.9	14.4	14.1	14.2	9.6	9.8	9.7	11.8	11.7	11.7
5	9.7	9.6	9.6							12.1	11.7	11.9	12.8	12.7	12.8	9.6	9.8	9.7	12.5	11.5	12.0
6	13.4	12.8	13.1							13.8	12.0	12.9	13.4	13.2	13.3	12.6	12.3	12.5	12.5	14.3	13.4
7	9.8	9.6	9.7							12.2	11.7	11.9	14.0	13.2	13.6	10.1	10.5	10.3	13.4	12.4	12.9
8	12.3	12.0	12.1													14.5	12.7	13.6	12.9	12.0	12.5
9	14.1	13.8	13.9													12.9	11.8	12.4			
10	10.5	10.5	10.5													11.9	11.2	11.6			
11	13.1	13.1	13.1													13.6	13.2	13.4			
12	9.3	9.5	9.4																		

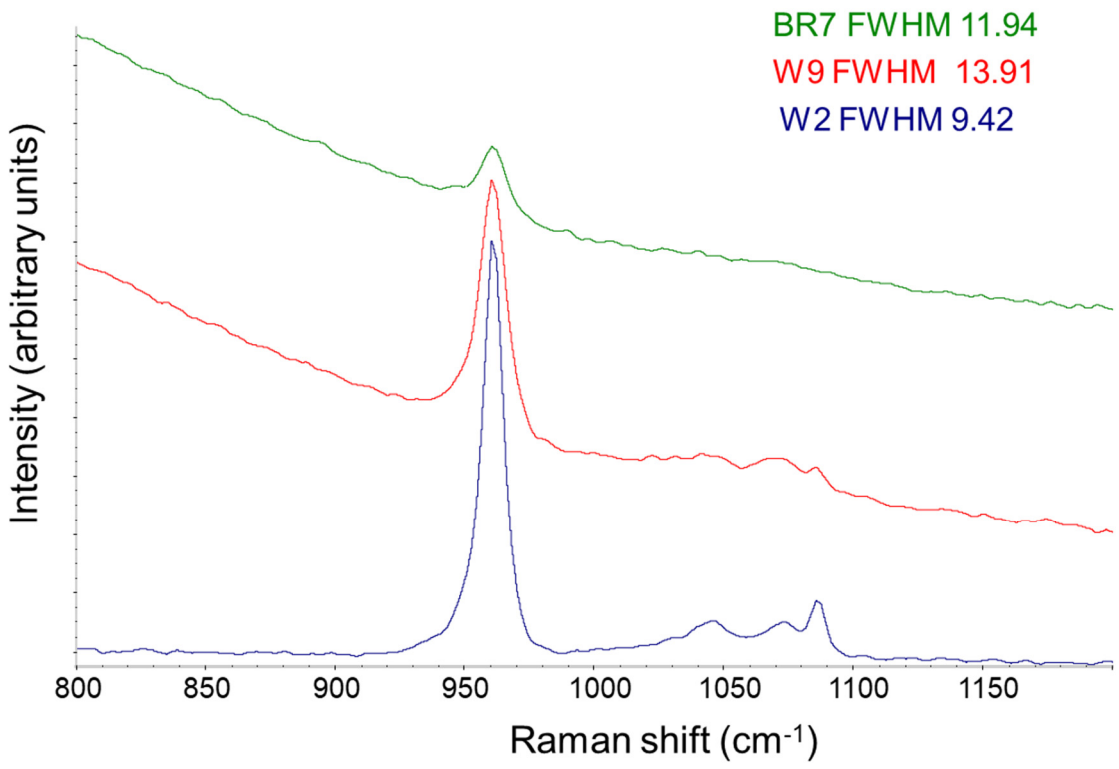

(**a**)

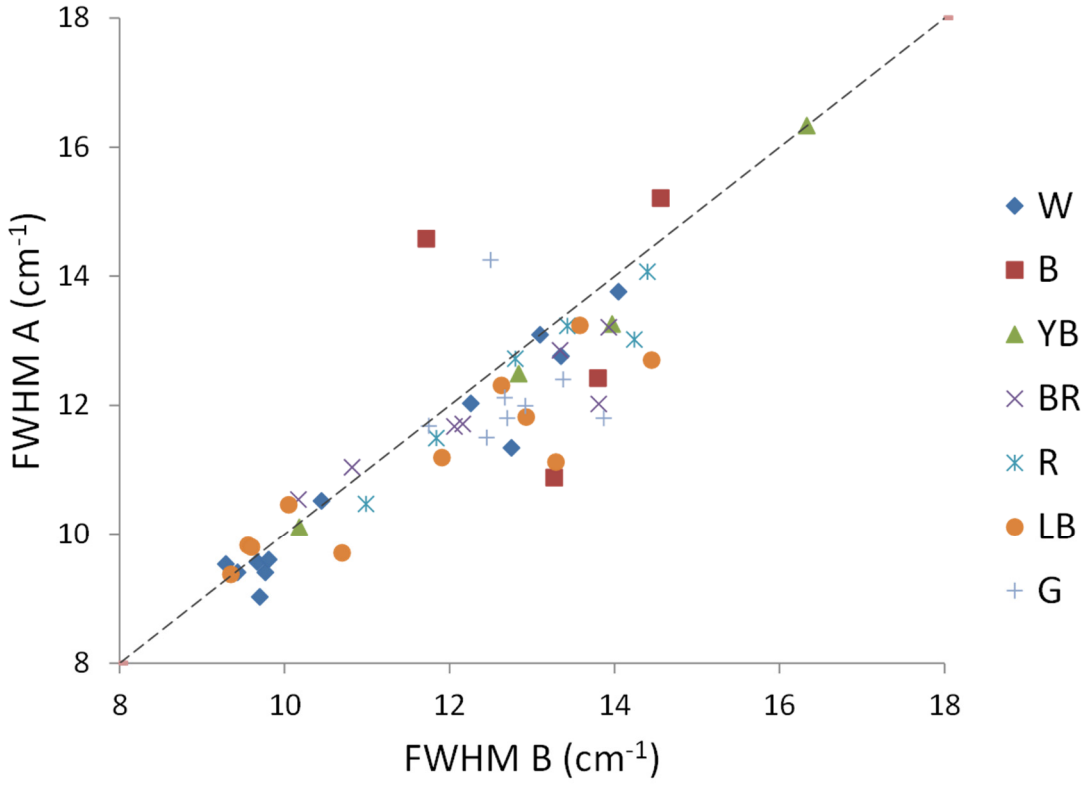

(**b**)

Figure 2. (**a**) Raman spectra of BR7 (green), W9 (red), and W2 (blue) in the region of the $\nu_1(PO_4^{3-})$ vibration at, 960 cm^{-1} showing different FWHM for the different samples. (**b**) Correlation between determination sets (A and B) of FWHM of the 960 cm^{-1} Raman line. Correlation coefficient is 0.880.

We then compared the classification based on the color to that based on the CI value determined from Raman spectra. In Figure 3 we report the average values of the FWHM of the 960 cm^{-1} band and the calculated CI together with the color label assigned prior to grinding.

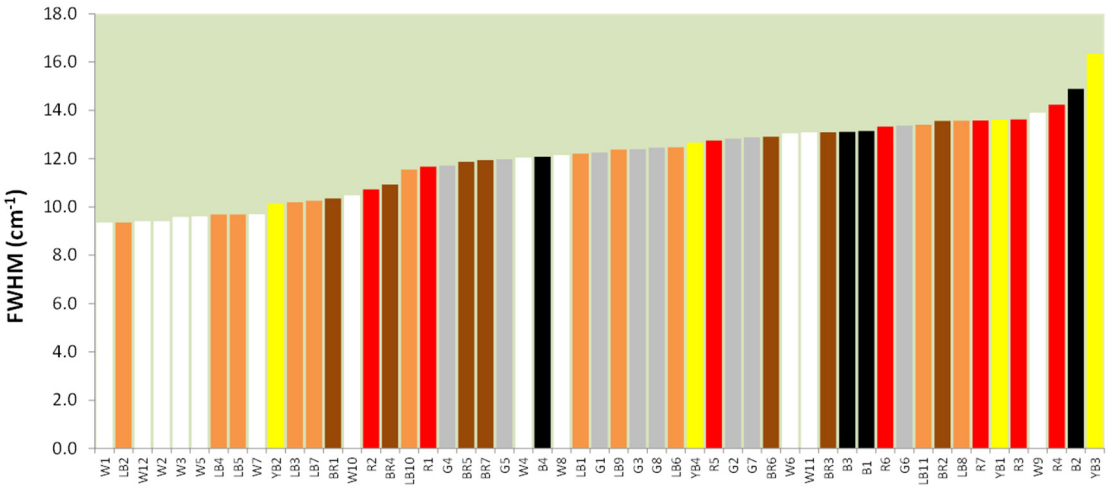

Figure 3. Histogram showing the FWHM of all samples ordered according to increasing FWHM. Colors refer to the labels assigned to the samples.

The analysis of the data shows that most of the white samples, as expected, have the smallest FWHM (≅9 cm^{-1}) and therefore the largest CI, however, there are also white samples with a much larger FWHM. By the same token we see that there are samples labeled with different colors which have a similar FWHM. As for the largest FWHM (13–14 cm^{-1}), likely the less crystalline samples, there is no dominant coloration suggesting that temperature is not the only relevant event affecting crystallinity. Probably, the presence of impurities such as adsorbed ions during burial time might induce a number of modifications both in composition and structure. These observations support the fragility of a classification based just on the color, at least for archaeological samples.

As for the infrared analysis probably the most widely used marker is the splitting factor of the doublet previously defined. A higher value of SF corresponds to a more crystalline sample and hence to a smaller Raman CI (reciprocal of the 960 cm^{-1} FWHM).

As far as SF is concerned, SF values are low in modern, unaltered bones (SF = 2.5–2.9) and very high in burnt bones or those affected by severe diagenesis (SF ~ 7) [21,24–26].

SF can be obtained either by using absorption IR (SF-IR) or ATR (SF-ATR) spectra. As previously explained, both techniques have critical aspects. Indeed, as it can be seen in Figure 4, if we compare the SF values obtained with the two approaches the correlation is not very good.

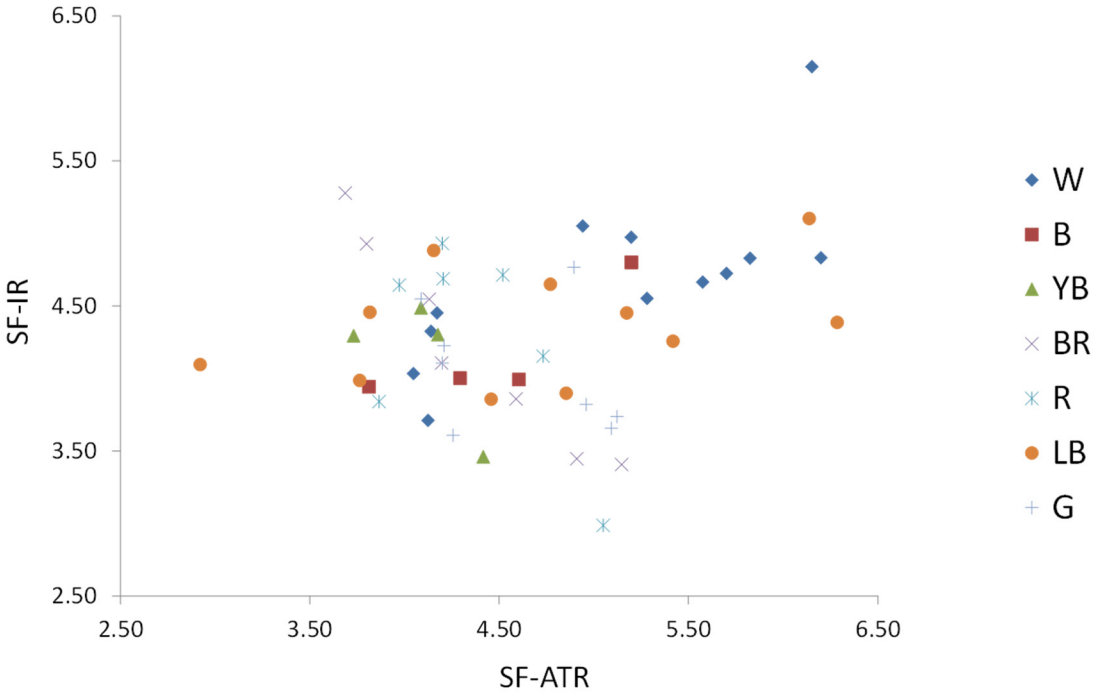

Figure 4. Correlation between SF-IR and SF-ATR values. Correlation coefficient is 0.673.

Which one of the two spectroscopic techniques is more reliable is an open issue. We believe that intensity determinations are more reliable using IR absorption.

In order to judge on the correlation between SF and Raman-CI in Figure 5a we plot SF-IR vs. Raman CI and in Figure 5b SF-ATR vs. Raman CI. It is apparent that in the former case we obtain a better correlation.

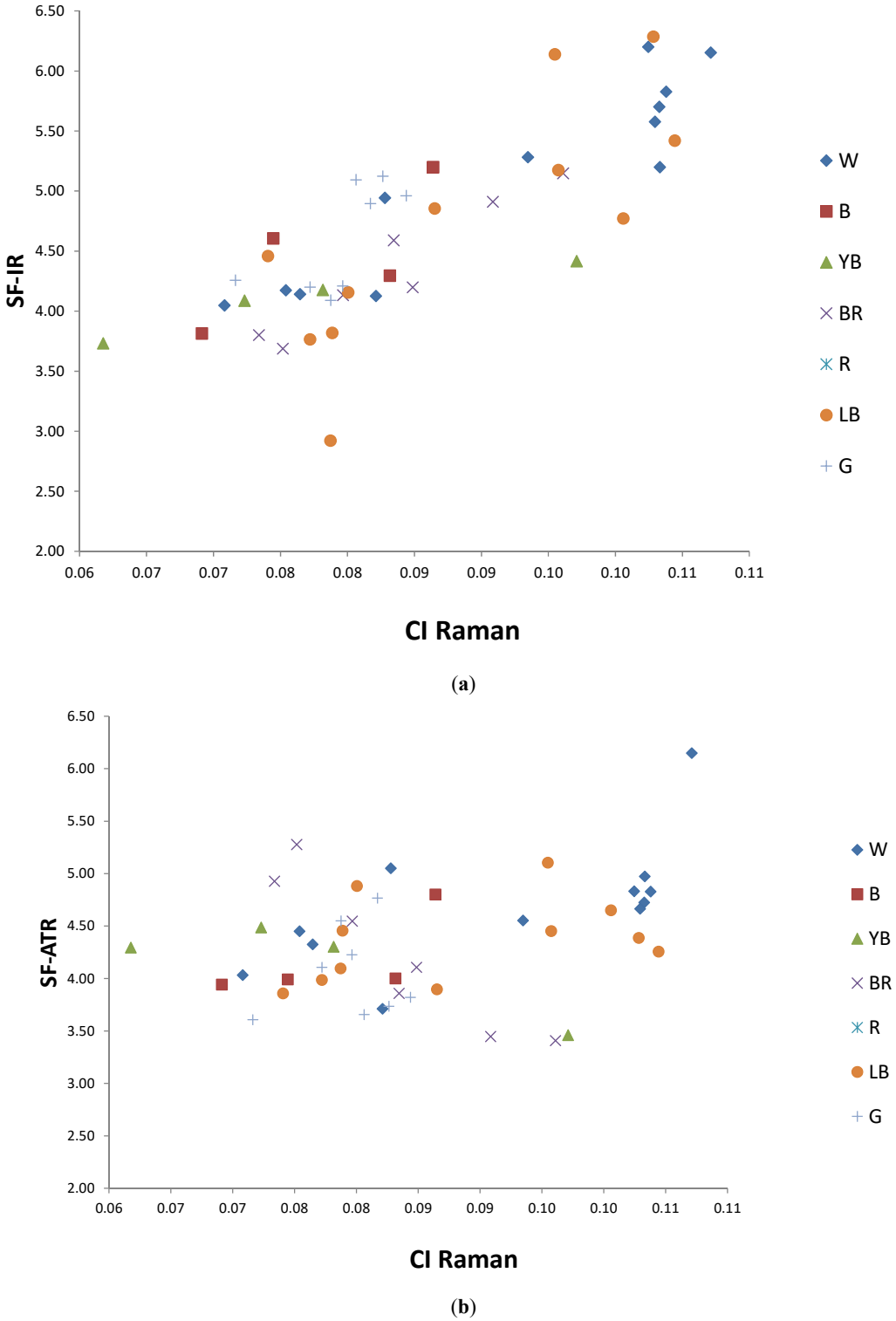

Figure 5. (**a**) Correlation between SF-IR and Raman CI. Correlation coefficient is 0,803. (**b**) Correlation between SF-ATR and Raman CI. Correlation coefficient is 0.644.

This finding is an indication that Raman CI values provide information consistent with that obtained with (SF-IR). As previously seen, Raman CI is known to correlate with the crystallinity determined with x-ray diffraction [5] and hence a correlation also between SF and CI (x-ray) might be expected.

Another observation in favor of the use of Raman CI as a possible marker of bone crystallinity is the following.

In the literature it has been observed that the heat induced reorganization of bioapatite's microcrystalline structure is revealed by the progressive narrowing of the bands upon increasing temperature coupled to the appearance of the characteristic signals from the hydroxyl groups OH libration and OH stretching at 630 cm^{-1} and 3570 cm^{-1} respectively [7].

The new band at 630 cm^{-1} appears to be related to the decomposition of the phosphates present in the sample [27] and it has been observed only when bones are exposed to temperature exceeding 700 °C or there has been severe diagenesis [5]. If this is correct, we expect to find a correlation between the intensity of this absorption band and Raman CI. We estimated the ratio between the integrated intensity of the bands at 630 cm^{-1} and 603 cm^{-1} (see Figure 6) and plotted it as a function of CI and we do observe some kind of correlation as it can be seen in Figure 7. Once again this suggests the reliability of using the Raman CI index as a marker for the study of bone crystallinity.

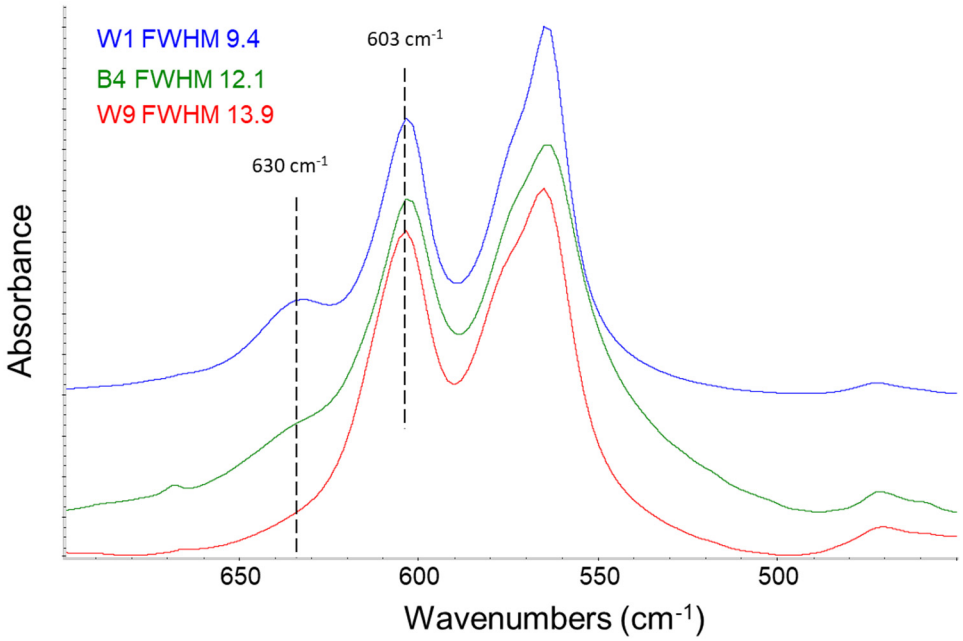

Figure 6. IR spectra of samples W1, B4, and W9 showing the appearance of the 630 cm^{-1} band in samples with smaller FWHM, i.e., in samples with a higher crystallinity.

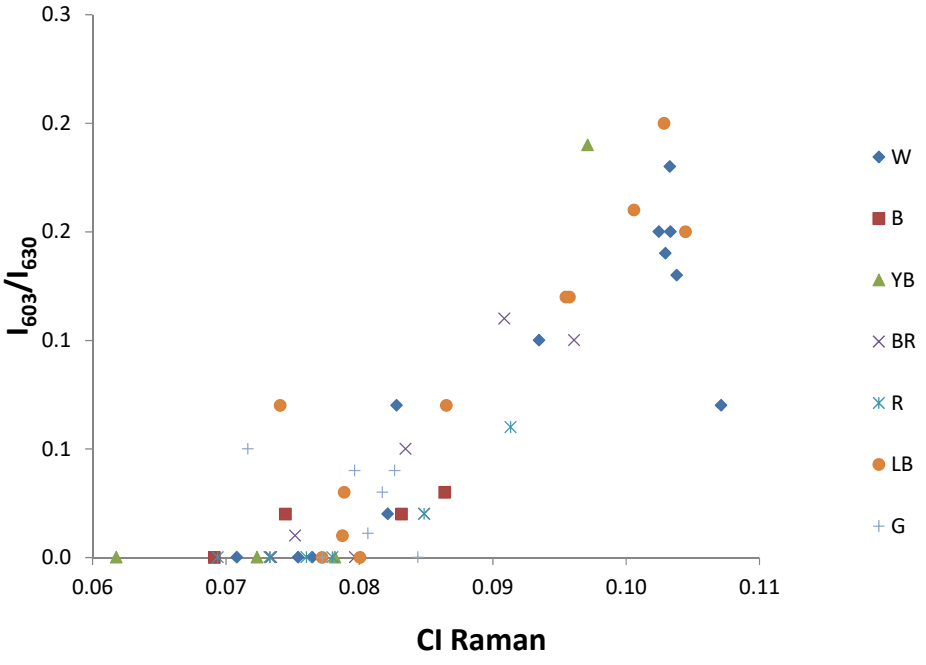

Figure 7. Comparison between the intensity ratio of the 630 cm^{-1} and 603 cm^{-1} IR absorptions and Raman CI. For samples with large FWHM values (i.e., less crystalline) the ratio is vanishingly small.

Moreover, as a further support to the use of this parameter, it has been verified that whenever the FWHM of the 960 cm^{-1} Raman band exceeds 13 cm^{-1} (less crystalline) no band (or negligibly small) at 630 cm^{-1} is observed.

4. Conclusions

In this work we presented a vibrational spectroscopy study on burned bones from an archaeological excavation site. The identification of reliable spectroscopic markers that can be used to reveal the history of burned bones is extremely useful in a variety of situations ranging from archaeological studies to forensic applications. However, due to the complex nature of the remains to be analyzed and possible contaminations because of environmental effects, their use is not straightforward and unambiguous. For this reason, to reach a satisfactory level of accuracy, different approaches are needed. We have compared the reliability of the data obtained from ATR and transmission FTIR measurements and we think we can say a word in favor of the use of FTIR in spite of some issues related to the sample preparation. Moreover, we suggest that also Raman spectroscopy can be a valuable characterization technique due to the ease of sampling and the existence of reliable spectroscopic markers. Another rather unique advantage of the Raman technique is that it can be used also for "*in situ*" analysis, an approach that, given the aforementioned applications, might reveal itself extremely useful.

The combined use of IR and Raman spectroscopies, together with other techniques (XRD; INS, etc.) can shed light on the complex problem of characterizing burned bones. The specificity of each situation will suggest the optimal combination of the available markers to unravel the problem of interest.

Author Contributions

A.M.: Conceptualization, investigation, data curation. L.B.: Data curation, reviewing and editing. V.H.J.: Conceptualization. C.B.: Conceptualization. C.C.F.: Investigation. J.L.Z.: Investigation. M.D.Z.: Conceptualization, methodology, original draft preparation. All authors have read and agreed to the published version of the manuscript.

Funding

This research received no external funding.

Institutional Review Board Statement

Not applicable.

Informed Consent Statement

Not applicable.

Data Availability Statement

Not applicable.

Conflicts of Interest

The authors declare no conflict of interest.

Use of AI and AI-Assisted Technologies

No AI tools were utilized for this paper.

References

1. Wang, X.Y. Comparative study on inorganic composition and crystallographic properties of cortical and cancellous bone. *Biomed. Environ. Sci.* **2010**, *23*, 473–480.
2. Thompson, T.J.U.; Islam, M.; Bonniere, M. A new statistical approach for determining the crystallinity of heat-altered bone mineral from FTIR spectra J. *Archaeol. Sci.* **2013**, *40*, 416–422.
3. Thompson, T.J.U. Recent advances in the study of burned bone and their implications for forensic anthropology. *Forensic Sci. Int.* **2004**, *146*, S203–S205.
4. Etok, S.E.; Valsami-Jones, E.; Wess, T.J.; et al. Structural and chemical changes of thermally treated bone apatite. *J. Mater. Sci.* **2007**, *42*, 9807–9816.

5. Monge, G.; Carretero, M.I.; Pozo, M.; et al. Mineralogical changes in fossil bone from Cueva del Angel, Spain: Archaeological implications and occurrence of whitlockite. *J. Archaeol. Sci.* **2014**, *46*, 6–15.
6. Ellingham, S.T.; Thompson, T.J.; Islam, M.; et al. Estimating temperature exposure of burnt bone—A methodological review. *Sci. Justice* **2015**, *55*, 181–188.
7. Marques, M.P.; Mamede, A.P.; Vassalo, A.R.; et al. Heat-Induced Bone Diagenesis Probed by Vibrational Spectroscopy. *Sci. Rep.* **2018**, *8*, 15935.
8. Thompson, T.J. An investigation into the internal and external variables acting on crystallinity index using Fourier Transform Infrared Spectroscopy on unaltered and burned bone. *Palaeogeogr. Palaeoclimatol. Palaeoecol.* **2011**, *299*, 168–174.
9. Mamede, A.P.; Gonçalves, D.; Marques, M.P.; et al. Burned Bones Tell Their Own Stories: A Review of Methodological Approaches to Assess Heat-Induced Diagenesis*. Appl. Spectrosc. Rev.* **2018**, *53*, 603–635.
10. Nakano, T.T. Variation in crystallinity of hydroxyapatite and the related calcium phosphates by mechanical grinding and subsequent heat treatment. *Metall. Mater. Trans. A* **2002**, *33*, 521–528.
11. Paschalis, E.B. FTIR micro-spectroscopic analysis of normal human cortical and trabecular bone. *Calcif. Tissue Int.* **1997**, *61*, 480–486.
12. Mkukuma, L.D.; Skakle, J.M.S.; Gibson, I.R.; et al. Effect of the proportion of organic material in bone on thermal decomposition of bone mineral: an investigation of a variety of bones from different species using thermogravimetric analysis coupled to mass spectrometry, high-temperature X-ray diffraction, and Fourier transform infrared spectroscopy. *Calcif. Tissue Int.* **2004**, *75*, 321–328.
13. Person, A.B. Early diagenetic evolution of bone phosphate: An X-ray diffractometry analysis. *J. Archaeol. Sci.* **1995**, *22*, 211–221.
14. Shemesh, A. Crystallinity and diagenesis of sedimentary apatites. *Geochim. Cosmochim. Acta.* **1990**, *54*, 2433–2438.
15. Weiner, S.; Bar-Yosef, O. States of preservation of bones from prehistoric sites in the Near East: A survey. *J. Archaeol. Sci.* **1990**, *17*, 187–196.
16. Querido, W.; Ailavajhala, R.; Padalkar, M.; et al. Validated Approaches for Quantification of Bone Mineral Crystallinity Using Transmission Fourier Transform Infrared (FT-IR), Attenuated Total Reflection (ATR) FT-IR, and Raman Spectroscopy. *Appl. Spectr.* **2018**, *72*, 1581–1593.
17. Wojdyr, M. Fityk: A general-purpose peak fitting program. *J. Appl. Cryst.* **2010**, *43*, 1126–1128.
18. Ruíz, C.B.; Ortega, D.B.; Caparrós, M.; et al. The Cueva del Angel (Lucena, Spain): An Acheulean hunters habitat in the South of the Iberian Peninsula. *Quat. Int.* **2011**, *243*, 105–126.
19. Shipman, P.F. Burnt bones and teeth: An experimental study of color, morphology crystal structure and shrinkage. *J. Archaeol. Sci.* **1984**, *11*, 307–325.
20. Nicholson, R. A morphological investigation of burnt animal bone and an evaluation of its utility in archaeology. *J. Archaeol. Sci.* **1993**, *20*, 411–428.
21. Stiner, M.C.; Kuhn, S.L.; Weiner, S.; et al. Differential burning, recrystallization, and fragmentation of archaeological bone. *J. Archaeol. Sci.* **1995**, *22*, 223–237.
22. Schiegl, S.; Goldberg, P.; Bar-Yosef, O.; et al. Ash deposits in Hayomin and Kebara caves, Israel: Macroscopic, microscopic and mineralogical observations and their archaeological implications. *J. Archaeol. Sci.* **1996**, *23*, 763–781.
23. Stiner, M.C.; Kuhn, S.L.; Surovell, T.A. Bone preservation in Hayomin Cave (Israel): A macroscopic and mineralogical study. *J. Archaeol. Sci.* **2001**, *28*, 643–659.
24. Shahack-Gross, R.; Bar-Yosef, O.; Weiner, S. Black-coloured bones in Hayomin Cave, Israel: Differentiating between burning and oxide staining. *J. Archaeol. Sci.* **1997**, *24*, 439–446.
25. Weiner, S.G. Bone preservation in Kebara Cave, Israel using on-site fourier transform infrared spectrometry *J. Archaeol. Sci.* **1993**, *20*, 613–628.
26. Schiegl, S.G. Paleolithic burnt bone horizons from the Swabian Jura: Distinguishing between *in situ* fireplaces and dumping areas. *Geoarchaeol. Int. J.* **2003**, *18*, 541–565.
27. Thompson, T.J.; Gauthier, M.; Islam, M. The Application of a New Method of Fourier Transform Infrared Spectroscopy to the Analysis of Burned Bone. *J. Archaeol. Sci.* **2009**, *36*, 910–914.